Fragility in *p*-spin models

G. Parisi,[1,2] G. Ruocco,[1,3] and F. Zamponi[1,*]

[1]*Dipartimento di Fisica and INFM, Università di Roma La Sapienza, P. A. Moro 2, 00185 Roma, Italy*
[2]*INFM - CRS SMC, Università di Roma La Sapienza, P. A. Moro 2, 00185 Roma, Italy*
[3]*INFM - CRS Soft, Università di Roma La Sapienza, P. A. Moro 2, 00185 Roma, Italy*

We investigate the relation between fragility and phase space properties — such as the distribution of states — in the mean-field *p*-spin model, a solvable model that has been frequently used in studies of the glass transition. By direct computation of all the relevant quantities, we find that (i) the recently observed correlation between fragility and vibrational properties at low temperature is present in this model and (ii) the total number of states is a decreasing function of fragility, at variance with what is currently believed. We explain these findings by taking into account the contribution to fragility coming from the transition paths between different states. Finally, we propose a geometric picture of the phase space that explains the correlation between properties of the transition paths, distribution of states, and their vibrational properties. However, our analysis may not apply to strong systems where inflection points in the configurational entropy as a function of the temperature are found.

I. INTRODUCTION

The glass-forming materials are characterized by a huge variation of their transport (viscosity, mobility, diffusivity) and dynamical (relaxation times) properties, upon supercooling. As an example, the viscosity in the whole "liquid" range, if crystallization is avoided, increases of about 17 orders of magnitude by decreasing the temperature before the system falls in the glassy state. The transition to the latter is conventionally fixed at the temperature T_g where the viscosity reaches a value of $10^{13} P$. Different systems show different temperature behavior of the viscosity, and they have been classified accordingly. Fragility is an index measuring the steepness of the viscosity as a function of the temperature on approaching the glassy state: "fragile" systems (high value of the fragility index) are characterized by a super-Arrhenius behavior of the viscosity, which increases very fast and—if extrapolated below T_g—seems to diverge at a finite temperature T_K. In "strong" systems (low value of the fragility index), on the contrary, the viscosity increase is less dramatic and follows an Arrhenius law, apparently diverging only at zero temperature.

The identification of the microscopic details that, in a given glass former, determine the temperature dependence of the viscosity, and thus the value of the fragility, is a long-standing issue in the physics of supercooled liquids and the glassy state. Large numerical and theoretical efforts have been devoted to the attempt to relate the fragility to specific interparticle interactions (e.g., strong glasses are often characterized by highly directional covalent bonds, while the fragile ones have more or less isotropic interactions). More recently, the attention has been focused on the possible relation existing between the fragility and features of the potential energy landscape (PEL), more specifically the energy distribution of the minima of the PEL and the properties of

the basin of attractions of such minima. With this respect, a key point is the existence of a relation between viscosity (or relaxation times) and the configurational entropy $\Sigma(T)$ (i.e., the number of basins populated at a given temperature): namely, the Adam-Gibbs relation

$$\eta(T) = \eta_\infty \exp\left(\frac{\mathcal{E}}{T \Sigma (T)}\right). \quad (1)$$

Here $\eta(T)$ is the viscosity and η_∞ its high-temperature limit. This relation has been extensively tested against experimental results, and it is now commonly accepted as "correct". Despite its success in describing both numerical and experimental data, the Adam-Gibbs relation still has not been derived in a clear way from microscopic models. This leaves unsolved the question of the microscopic interpretation of the parameter $\mathcal{E}$, which is usually believed to be related to the properties of the transition paths between different minima of the potential energy, such as the height of the barriers or the connectivity of the minima. By using the Adam-Gibbs relation, one could expect to relate fragility to the properties of $\Sigma(T)$ —i.e., to the distribution of basins in the phase space of the system. However, this possibility is frustrated by the lack of knowledge of the parameter $\mathcal{E}$. Indeed, once a model for $\Sigma(T)$ has been chosen, one can obtain the whole range of experimentally observed fragilities by varying $\mathcal{E}$ (see Ref. [1] and references therein). More specifically, in Ref. [1] it was observed that for a large class of models for $\Sigma(T)$ — where $\Sigma(T)$ is a concave function of T that vanishes at a given temperature T_K and assumes its maximum Σ^* at high temperature ("Gaussian-like models") — the relevant parameter that actually determines the fragility is

$$D = \frac{\mathcal{E}}{T_K\Sigma^*}. \quad (2)$$

Thus, fragility appears to be determined by the ratio between $\mathcal{E}$ (measured in units of $k_B T_K$) and the total number of states

*Electronic address: francesco.zamponi@phys.uniroma1.it

Σ^*/k_B; it is related to both the distribution of minima (through Σ^*) and the characteristic of the transition path between them (through $\mathcal{E}$). The relation between fragility and phase space properties can be even more complicated in those cases where the function $\Sigma(T)$ does not belong to the Gaussian class.

The relevance of the concept of fragility also relies on the correlations that have been found between this index and other properties of glass-forming liquids. Examples of these correlations are the specific heat jump at T_g (thermodynamic fragility) [2], the degree of stretching in the nonexponential decay of the correlation functions in the liquid close to T_g [3], the visibility of the boson peak at the glass transition temperature [4], or the temperature behavior of the shear elastic modulus in the supercooled liquid state [5]. More recently a striking correlation between fragility and the vibrational properties of the glass at low temperatures has been found [6]. Specifically, by examining the dynamic structure factors of different glass formers well below T_g, it has been found that the fragility of the corresponding liquid is proportional to the rate of change of the nonergodicity factor in the $T \rightarrow 0$ limit. The latter quantity being fully determined by the (harmonic) vibrational properties (eigenmodes of the disordered structure), this finding implies the existence of a deep relation between three features of the PEL: the energy of the minima, the transition paths between them (that together determine the fragility), and the Hessian matrix, evaluated at the minima themselves, which fixes the vibrational properties.

With the aim to elucidate the existence of this unexpected correlation between energy, curvature, and transition paths in the minima of the PEL we selected a solvable model of "glass," where (i) the distribution of minima is "Gaussian like," (ii) the vibrational properties of the minima can be determined, and (iii) the transition path between different minima can be evaluated and characterized by an energy parameter. More specifically, we investigate the mean-field p-spin model (in both its spherical and Ising spin versions), a model that shares with the structural glasses many aspects of the glass transition phenomenology and that is known to have a Gaussian-like distribution of states. Our goal is twofold: (i) we aim to verify if the analysis reported in [1] is indeed correct in some microscopic model — i.e., if one can obtain a wide range of fragilities in a Gaussian-like model by varying the parameter ε—and (ii) to check whether one can explain the correlation between fragility of the liquid and the vibrational properties of its glass found in [6] by studying the geometry of the phase space. The latter point could allow us to shed light on the origin of the correlation between number of minima, their vibrational properties, and the property of the transition path between them.

The paper is organized as follows: in Sec. II we define the relevant quantities in the case of the mean-field p-spin model; in Sec. III we compute them for the spherical p-spin model and in Sec. IV for the Ising p-spin model; in Sec. V we discuss the relation between fragility and phase space geometry in these models and compare our result with experimental data. Finally, we draw the conclusions.

II. DEFINITION OF THE RELEVANT OBSERVABLES

The quantities we wish to compute are

T_K	thermodynamical transition temperature;
T_g	glass transition temperature;
T_d	dynamical transition temperature;
$\Sigma(T_g)$	complexity at T_g;
$m(T_g)$	fragility;
$\alpha(T_g)$	"volume" of the equilibrium states at T_g;
$\mathcal{E}(T_g)$	"barrier height" at T_g;

Setting $k_B=1$, all the above quantities are either dimensionless or have the dimension of an energy; in the p-spin model—as usual in classical spin models—a natural energy scale J appears as the strenght of the couplings between spins. Thus, if we additionally set $J=1$, all the quantities we will deal with in this paper become dimensionless; in the following, with this specification, we will always deal with dimensionless quantities.

We have now to identify the proper definition of these quantities in a mean-field model. The main problem is that in a mean-field model the glass transition temperature T_g is not a well-defined quantity. Indeed, the relaxation time of the system is known to diverge — as a power law — when the temperature approaches the dynamical transition temperature T_d, which corresponds to the usual mode-coupling temperature T_{MCT}. The crossover from a power-law behavior of the relaxation time to an Arrhenius-like behavior, observed around T_{MCT} in finite-dimensional systems, is due to the activated processes becoming relevant; these processes are absent in mean-field systems, and the crossover at T_{MCT} becomes a true dynamical transition at T_d [7]. To overcome this problem, we will give an estimate of the height $\mathcal{E}(T)$ of the barrier that the system must pass through in order to escape from a metastable state at a given temperature T. Thus, we will make use of a "fictitious" Adam-Gibbs relation

$$\eta(T) = \eta_\infty \exp\left(\frac{\mathcal{E}(T)}{T \Sigma(T)}\right) \qquad (3)$$

and define T_g by $\eta(T_g)/\eta_\infty = \text{const}$ or, equivalently, by

$$\frac{\mathcal{E}(T_g)}{T_g \Sigma(T_g)} = \text{const}. \qquad (4)$$

Note that in this paper we will not distinguish between the "complexity" (or "configurational entropy") $\Sigma(T)$, which can be calculated in mean-field models, and the "excess entropy" measured in the experiments: indeed, they behave in a similar way in a wide class of systems [8]. Obviously, the quantity $\eta(T)$ has no dynamical meaning in a mean-field context, but it provides a useful definition of T_g that hopefully coincides with the usual one in finite dimensions. It will turn out that our analysis is not strictly dependent on this definition of T_g, the behavior of the various quantities at T_g being representative, as we will see, of a general trend observed at all temperatures $T \, \mathcal{E} \, [T_K, T_d]$ by varying p.
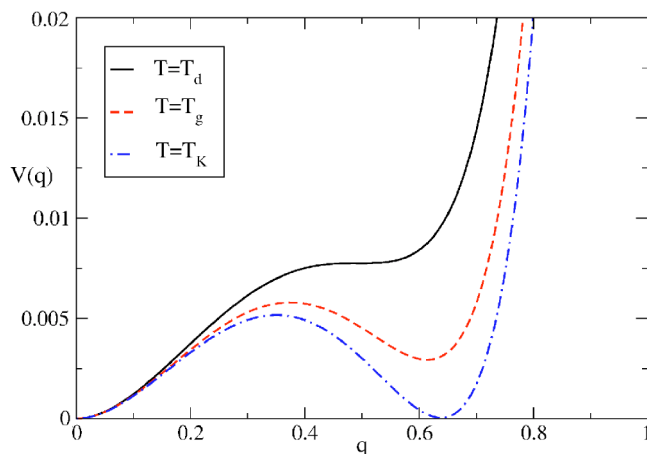
FIG. 1. The two-replica potential for $T \in [T_K, T_d]$ in the spherical p-spin model.

A. Two-replica potential

The easiest way to provide a definition of all the above quantities is to consider the two-replica potential approach introduced and discussed in [9,10]. This function $V(q,T)$ can be interpreted as the free-energy cost paid to keep two copies of the system at a fixed overlap q:

$$V(q,T) = F_q(T) - F_0(T); \qquad (5)$$

here $F_q(T)$ is the free energy of two copies of the system when constrained to have fixed overlap q, and $F_0(T) = 2F(T)$ is the free energy of two independent copies of the system.

Its qualitative behavior is shown in Fig. 1 for the one step replica symmetry breaking (1RSB) mean-field p-spin spherical model: for $T > T_d$ it is a convex function of q with only one minimum at $q=0$. At the dynamical transition temperature T_d a secondary minimum starts to develop at finite q. On lowering the temperature below T_d, the value of V at the minimum decreases and vanishes at the thermodynamical transition temperature T_K.

From the potential $V(q,T)$ one can extract information about the complexity $\Sigma(T)$ and the barrier height $\mathcal{E}(T)$. Indeed, it is well known that for $T_K < T < T_d$ the phase space of 1RSB models is disconnected in an exponentially high number of metastable states. The Gibbs equilibrium state is a superposition of a subset of these states ("equilibrium states") having a defined self-overlap $q(T)$; however, the probability of finding — at equilibrium — two independent copies of the system in the same state is zero [11]. Different states have zero overlap; we therefore expect that the stable phase of the two copies of the system — i.e., the one for which $V(q)$ is minimum — is at $q=0$. This is indeed the case as one can see from Fig. 1. The secondary minimum at $q \neq 0$ can then be interpreted as a metastable state for the two coupled systems, which corresponds to the situation where both systems are in the same state with self-overlap $q(T)$. Thus, the value $q_{min}(T)$ where $V(q,T)$ has a secondary minimum can be interpreted as the self-overlap of the equilibrium states at temperature T.

The free energy of the system for $T_K < T < T_d$ can be written as

$$F(T) = f(T) - T\Sigma(T), \qquad (6)$$

where $f(T)$ is the free energy of a single equilibrium state at temperature T and $\Sigma(T)$ is the complexity—i.e., the logarithm of the number of equilibrium states. The free energy of two independent copies of the system is $F_0(T) = 2F(T) = 2f(T) - 2T\Sigma(T)$, while the free energy of two copies constrained to be in the same equilibrium state is given by

$$F_{q_{min}}(T) = 2f(T) - T\Sigma(T). \qquad (7)$$

Thus,

$$V(q_{min},T) = F_{q_{min}}(T) - F_0(T) = T\Sigma(T), \qquad (8)$$

and the equilibrium complexity $\Sigma(T)$ can be deduced from the function $V(q,T)$.

The difference between the value of V at the maximum and the value of V at the minimum can be interpreted as the height of a "barrier" that the two coupled systems have to overcome to escape from the situation where they are constrained to be in the same state. Thus, we can define the "barrier height" $\mathcal{E}(T) = V(q_{max},T) - V(q_{min},T)$. Note that a system-dependent proportionality factor is needed in order to account for the cooperativity of the process of escaping from a state: indeed, $V(q)$ is the free energy per spin, while an unknown number of spins can be involved in the escaping process. Therefore, the $\mathcal{E}(T)$ defined above is an estimate of the barrier height up to an unknown (system-dependent) proportionality factor.

B. Temperatures

The thermodynamical transition temperature T_K is defined as the temperature where the complexity vanishes: $\Sigma(T_K) = 0$. Then, at T_K the value of V at the secondary minimum becomes equal to zero (see Fig. 1). The dynamical transition temperature T_d is the temperature at which the metastable minimum first appears. We now provide a definition of the "glass transition temperature" T_g. As we discussed at the beginning of this section, using the Adam-Gibbs relation, the usual definition of glass transition temperature turns out to be

$$\frac{\mathcal{E}(T_g)}{T_g \Sigma(T_g)} = \mathcal{C}. \qquad (9)$$

The value of the constant $\mathcal{C}$ is arbitrary. Taking into account the fact that in the considered models $\mathcal{E}$ is defined up to a proportionality factor, we can fix the value of the constant in order to obtain reasonable (with respect to experiments) values for the different quantities we want to study, fragility in particular. Different choices of the constant change only quantitatively the results, while the qualitative picture stays the same.

C. Complexity, barrier heights, and fragility

Given a definition of T_g, the complexity at T_g is simply $\Sigma(T_g)$ and the barrier height $\mathcal{E}(T_g)$: clearly, these two quan-
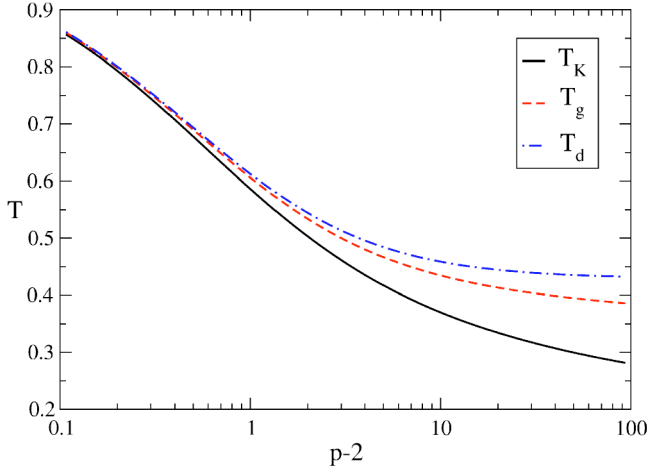
FIG. 2. Thermodynamic transition temperature T_K, glass transition temperature T_g and dynamical transition temperature T_d for the p-spin spherical model as a function of $p-2$.

tities are related by Eq. (9). Knowing the complexity as a function of the temperature, we can define the fragility as

$$m(T_g) = 1 + T_g \frac{\Sigma'(T_g)}{\Sigma(T_g)}. \tag{10}$$

The latter definition is very useful in a mean-field context as — once a definition of T_g has been chosen — it involves only the complexity, which is a well-defined quantity in mean-field models. It is equivalent to the usual Angell definition of fragility if η_∞=const, and the Adam-Gibbs relation is assumed to be valid [1]. This definition of fragility has been shown to be related to the one usually considered in experiments in Ref. [2].

D. Volume of the states

As we discussed in the Introduction, in Ref. [6] fragility has been shown to be correlated with an index related to the volume of the states populated at equilibrium around T_g. More precisely, in [6] this index has been defined as

$$\alpha(T_g) = \lim_{k\to 0} \left. \frac{d[f_k(T)]^{-1}}{d(T/T_g)} \right|_{T=0}, \tag{11}$$

where $f_k(T)$ is the nonergodicity factor extracted from the dynamic structure factor $S(k,\omega)$ at a given wave vector k. From Fig. 2 of Ref. [6], we see that the possibility of classifying the considered systems in term of α — given by Eq. (11) — relies on the observation that the curves of f_k as a function of T/T_g for different systems do not intersect [the same observation, which holds for $\ln \eta(T)$ as a function of T_g/T, is the basis of the definition of fragility]. Therefore, the index α defined in [6] can be replaced by other equivalent — by equivalent we mean positively correlated — definitions (like the definition of $F_{1/2}$ as a "fragility index" [2]). An useful equivalent definition of α is

$$\alpha(T_g) = \lim_{k\to 0}[1 - f_k(T_g)]. \tag{12}$$

As one can easily check observing Fig. 2 of Ref. [6], this definition is equivalent to Eq. (11) if the curves $f_k(T)$ do not intersect.

The quantity $f_k(T)$ (in the low-k limit) can be identified in the considered models with the self-overlap of the states: this identification comes from the observation that both quantities represent the *plateau* of a relevant correlation function. Thus, we will define

$$\alpha(T_g) = 1 - q(T_g), \tag{13}$$

where $q(T_g)$ is the self-overlap of the equilibrium states at T_g — i.e., the value of q where $V(q,T)$ has the secondary minimum at $T=T_g$ (see Fig. 1).

As the self-overlap of the states is related to their volume in phase space (high overlap corresponding to small states), a small value of α corresponds to small-volume states, while a big value of α corresponds to large-volume states. In this sense, $\alpha(T_g)$ will be called "volume of the equilibrium states at T_g." Note that a similar identification has been discussed in Ref. [6]: indeed, from Eq. (7) of Ref. [6] (note that due to a typographical error the power –1 has to be disregarded) one can see that α is related to the curvatures of the minima of the potential (in the harmonic approximation) and that small curvatures (large volume) correspond to large α, while high curvatures (small volume) correspond to small α. This is consistent with the equivalence of the definition of α given in Ref. [6] and the one adopted here.

E. Summary of the definitions

To conclude this section, we give a short summary of all the definitions we discussed. We will call $q_{min}(T)$ the value of q where $V(q,T)$ has the secondary minimum and $q_{max}(T)$ the value of q where $V(q,T)$ has a maximum. Then, we define

$$\Sigma(T) = V(q_{min}(T),T)/T,$$

$$\mathcal{E}(T) = V(q_{max}(T),T) - V(q_{min}(T),T),$$

$$T_K \quad : \Sigma(T_K) = 0,$$

$$T_g \quad : \frac{\varepsilon(T_g)}{T_g \Sigma(T_g)} = \mathcal{C},$$

$$T_d \quad : q_{max}(T_d) = q_{min}(T_d),$$

$$m(T_g) = 1 + T_g \frac{\Sigma'(T_g)}{\Sigma(T_g)},$$

$$\alpha(T_g) = 1 - q_{min}(T_g).$$

The constant $\mathcal{C}$ will be chosen in order for the fragility to be in the experimentally observed range.

III. SPHERICAL *p*-SPIN MODEL

In this section, we will compute explicitly all the previously defined quantities in the spherical *p*-spin model. The model is defined by the Hamiltonian

$$H_p = - \sum_{(i_1,\cdots,i_p)} J_{i_1,\cdots,i_p} \sigma_{i_1} \cdots \sigma_{i_p}, \qquad (14)$$

where σ_i are real variables subject to a spherical constraint $\Sigma_i \sigma_i^2 = N$, and $J_{i_1,\cdots,i_p}$ are quenched random Gaussian variables with zero mean and variance $p!/(2N^{p-1})$. This simple model has been successfully used for studies of the glass transition [7,12]. It is a "Gaussian-like" model, in the sense that its complexity — even if the distribution of states in not exactly Gaussian — is known to be a concave function of the temperature, which vanishes at T_K and assumes its maximum at T_d, without any inflection point in between [13].

The expression for $V(q,T)$ in the *p*-spin spherical model has been computed in Refs. [9,14]. However, a simplified expression can be used when the value of $V(q,T)$ *on its stationary points* is considered (see the Appendix):

$$V(q,T) = -\frac{\beta}{4} q^p - \frac{T}{2} \ln(1-q) - \frac{Tq}{2}. \qquad (15)$$

This function can be shown to coincide with the correct $V(q,T)$ on each stationary point of $V(q,T)$. As we are interested only in the value of $V(q,T)$ on its stationary points, the use of the correct $V(q,T)$ calculated in Refs. [9,14] or of the one given by Eq. (15) will give exactly the same result.

Note that, while the model is defined only for integer *p*, Eq. (15) holds also for real *p*; we will therefore discuss the behavior of the different quantities for any real $p \geqslant 2$. In particular, the $p \to 2$ limit is interesting being related to a diverging fragility ($T_d \to T_K$) and to the discontinuous 1RSB transition becoming a continuous one.

A. Temperatures

From Eq. (15) we can compute the three temperatures T_K, T_g, and T_d as functions of *p*. Their behavior is reported in Fig. 2. We immediately note that, for $p \sim 2$, the difference between T_K and T_g is very small therefore, the system is very fragile. Moreover, for $p \to \infty$ the Kauzmann temperature approaches zero (as $1/\sqrt{\ln p}$), while the glass transition temperature remains finite. The system therefore becomes stronger and stronger on increasing *p*.

B. Complexity and fragility

The same observation can be made more quantitative by considering an "Angell plot" for the complexity [2]: in Fig. 3 we show the complexity $\Sigma(T)$ as a function of temperature for different values of *p*. The choice of the particular scaling that appears in Fig. 3 has been made in order to make a close correspondence with Fig. 2 of Ref. [2]. We see that the curves for different values of *p* are ordered from bottom to top. The same behavior is observed in experimental systems of different fragility. Indeed, the index of fragility defined in
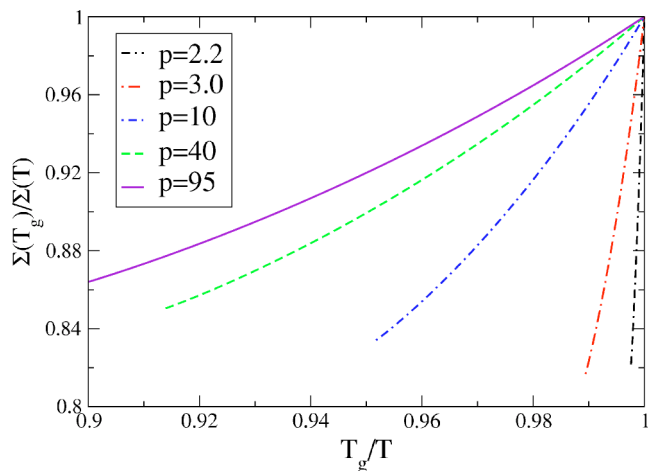

FIG. 3. The complexity $\Sigma(T_g)/\Sigma(T)$ as a function of T_g/T for the *p*-spin spherical model at different values of *p*. Fragility is the slope of the curves in $T_g/T = 1$. The system becomes stronger on increasing *p*.

Eq. (10) is exactly 1 plus the slope of the curves in $T_g/T = 1$ (see Fig. 3):

$$\begin{aligned} m(T_g) &= 1 + T_g \frac{\Sigma'(T_g)}{\Sigma(T_g)} \\ &= 1 + \left. \frac{d[\Sigma(T_g)/\Sigma(T)]}{d[T_g/T]} \right|_{T=T_g}. \end{aligned} \qquad (16)$$

The fragility index *m* is shown in Fig. 4 as a function of *p*. We see that it is a decreasing function of *p*. Its values are in the range observed for the experimental system due to our (arbitrary) choice of the constant $\mathcal{C}$ appearing in Eq. (9), $\mathcal{C} = 0.1$. In Fig. 4, $\Sigma(T_g)$ is also reported as a function of *p*. We see that it is an increasing function of *p*, which diverges as $\ln p$ for $p \to \infty$: thus, the number of states in this system is a decreasing function of the fragility, at variance with what is
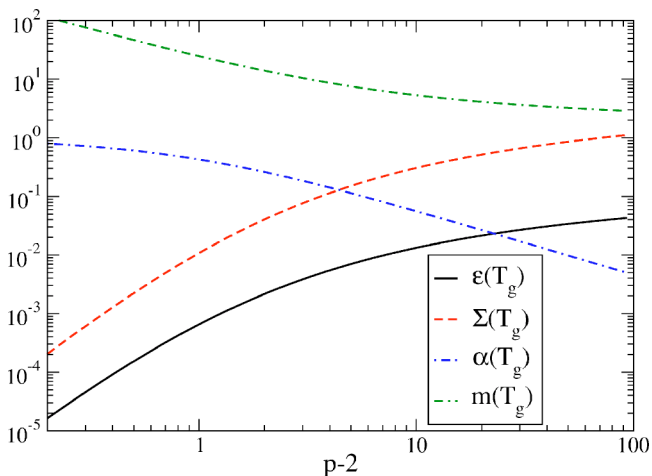

FIG. 4. Fragility $m(T_g)$, configurational entropy $\Sigma(T_g)$, "volume" of the equilibrium states $\alpha(T_g)$, and barrier height $\varepsilon(T_g)$ for the *p*-spin spherical model as a function of $p-2$.

currently believed (for a review, see Ref. [1]). We will discuss this point in detail in Sec. V.

C. Barrier heights and volume of the states

In Fig. 4 the barrier height $\mathcal{E}(T_g)$ is also reported as a function of p, together with the index $\alpha(T_g)=1-q(T_g)$, which we called the "volume" of the equilibrium states at T_g. We observe that in this model the states become smaller on increasing p, while the barriers separating them increase. In Sec. V we will discuss this behavior, trying to deduce a geometric description of the evolution of the phase space of this model at different p, and relate fragility to geometric properties of the phase space.

IV. ISING p-SPIN MODEL

The Ising p-spin model is another popular model for the study of the glass transition [15,16]. Its Hamiltonian is given by Eq. (14), where the variables σ_i are Ising spins, $\sigma_i=\pm 1$, and the spherical constraint is absent. For the Ising p-spin model, the two-replica potential $V(q,T)$ is given by

$$V(q,T) = \beta\frac{p-1}{4}q^p + \beta\frac{p}{4}q^{p-1} - \frac{\int \mathcal{D}z \, \cosh(\Lambda z)\ln \cosh(\Lambda z)}{\int \mathcal{D}z \, \cosh(\Lambda z)},$$

(17)

where $\mathcal{D}z=\exp(-z^2/2) \, dz$ and $\Lambda^2=\beta^2 pq^{p-1}/2$.

The Ising p-spin model is also a "Gaussian-like" model, like the spherical one. However, the total number of states in the Ising p-spin model cannot be greater than 2^N (the total number of configurations), and hence $\Sigma(T) \leq \ln 2$, while in the spherical model $\Sigma(T_g)$ diverges as $\ln p$ for $p \to \infty$, as previously discussed.

A. Temperatures

The first consequence of this difference is observed when studying the transition temperatures as a function of p (see Fig. 5). Indeed, as in the spherical model, we have $T_K \sim T_g$ for $p \sim 2$ and $T_g \gg T_K$ for $p \to \infty$. But in this model, T_K tends to a finite value at large p, while T_g and T_d diverge. This behavior can be understood recalling that for a "Gaussian-like" model we have $T_K \sim 1/\sqrt{\Sigma^*}$, Σ^* being the total number of states—i.e., the maximum of $\Sigma(T)$ [1].

B. Complexity and geometric properties of the phase space

The "Angell plot" for the complexity of the Ising p-spin model looks very similar to the one of the spherical model (see Fig. 3) and is not reported here.

Having fixed an appropriate value for the constant $\mathcal{C}$ in Eq. (9) ($\mathcal{C}=0.02$, different from the value chosen in the previous case), the behavior of the fragility as a function of p is also very similar to the one of the spherical model. The same behavior is found for the other quantities under study, as one can deduce from a comparison of Fig. 6 and 4, the main difference being the discussed behavior of $\Sigma(T_g)$ at large p.
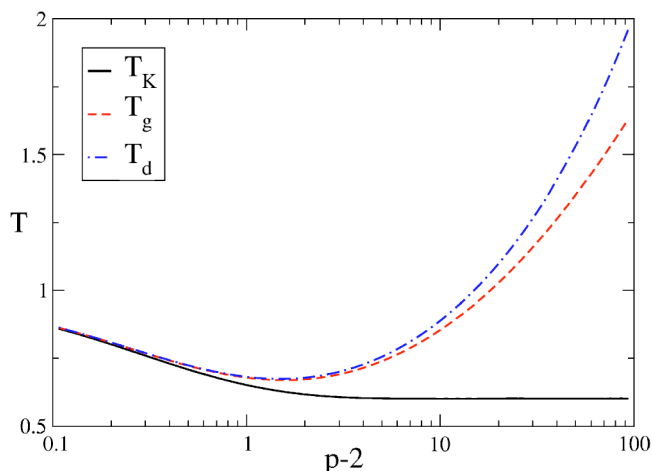

FIG. 5. Thermodynamic transition temperature T_K, glass transition temperature T_g, and dynamical transition temperature T_d for the p-spin Ising model as a function of $p-2$.

C. Vibrational properties and volume of the states

Another relevant difference between the spherical and Ising models is that, in the latter, harmonic vibrations are not present (the variables being discrete): we have $q(T) \to 1$ exponentially for $T \sim 0$, and the definition of α via Eq. (11) gives $\alpha=0$ for all p. However, the definition given in Eq. (13) and used in our calculations gives a reasonable result also in absence of harmonic vibrations.

V. CORRELATIONS BETWEEN DIFFERENT PROPERTIES OF THE PHASE SPACE

In this section we will examine the correlations in the quantities under study, trying to relate fragility to the phase space geometry. We will compare our results with the general considerations that we made in Ref. [1] and with the experimental results of Ref. [6].

A. Fragility and volume of the states

In Ref. [6] it has been established that fragility is positively correlated with the index α defined in Sec. II. In other
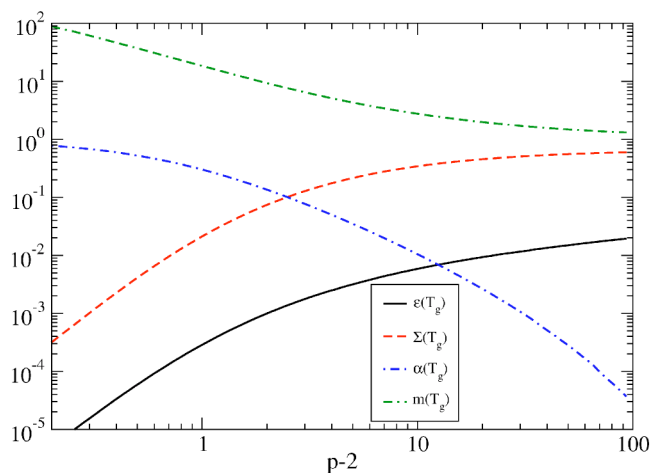

FIG. 6. Fragility $m(T_g)$, configurational entropy $\Sigma(T_g)$, "volume" of the equilibrium states $\alpha(T_g)$ and barrier height $\mathcal{E}(T_g)$ for the p-spin Ising model as a function of $p-2$.
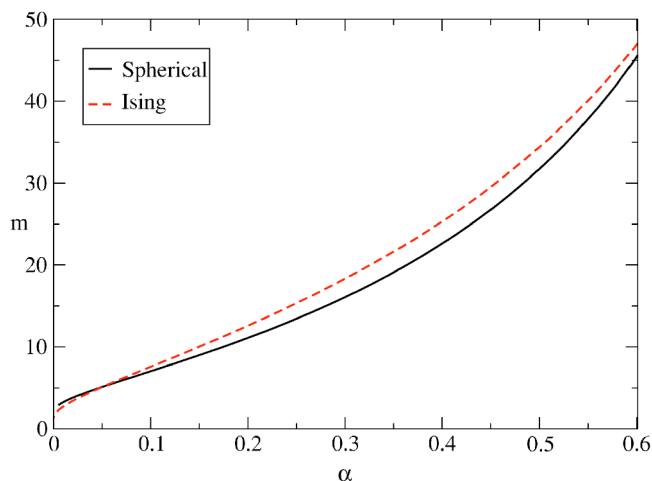
FIG. 7. Fragility versus α for the two investigated models. The curve is very similar for the two models and is consistent with the linear correlation found in [6] at least for $\alpha \lesssim 0.4$.
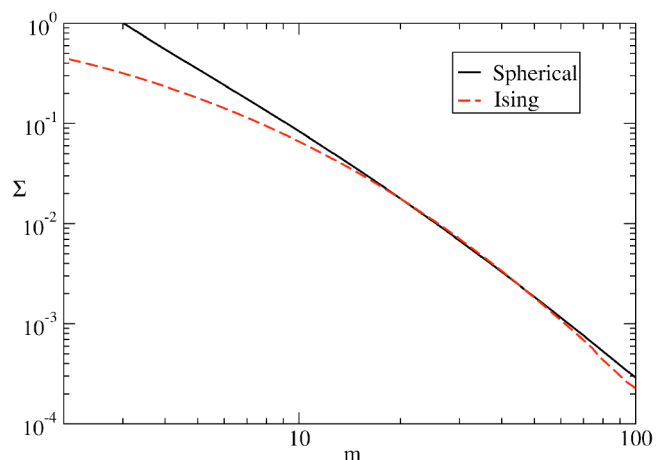

FIG. 8. Total number of states (represented by the complexity at T_g) as a function of the fragility m: an inverse correlation is found between these quantities, at variance with what is naively expected from the Adam-Gibbs relation.

words, *fragile systems have large basins while strong systems have small basins.* In Fig. 7 we plot the fragility m as a function of α parametrically in p for the investigated systems. The curve $m(\alpha)$ is very similar for the two models — remember that the only adjustable parameter is the constant $\mathcal{C}$ in Eq. (9). By comparison with Fig. 3 of Ref. [6], we conclude that the model has a behavior similar to the one of real systems. Surprisingly, also the linear correlation between m and α is reproduced for $\alpha \lesssim 0.4$. Thus, mean-field p-spin models are able to describe the relation between fragility and the volume of the basins visited around T_g found in Ref. [6].

B. Fragility and total number of states

It is usually believed that fragile systems have a larger number of states than strong ones, even if the total number of states is not an experimentally accessible quantity and numerical simulations give contradictory results [17]. However, in the model considered here the behavior is exactly the opposite. In Fig. 8 we report $\Sigma(T_g)$ as a function of the fragility: we see that the total number of states is a decreasing function of the fragility, at variance with what is currently believed. To discuss this point, we have to refer to [1]: there, we discussed the possibility of correlating fragility with the total number of states for general models of $\Sigma(T)$ and assuming the validity of the Adam-Gibbs relation, Eq. (1). We concluded that knowledge of the distribution of states is not enough to determine the fragility. Indeed, the relevant parameter was identified, for a general "Gaussian-like" distribution of states, as

$$D = \frac{\mathcal{E}(T_g)}{T_K \Sigma(T_g)}. \tag{18}$$

Note that in Eq. (18) we have to calculate $\mathcal{E}$ at $T = T_g$ because in the considered models the barrier height $\mathcal{E}$ is a T-dependent quantity, while in the Adam-Gibbs relation it is usually assumed to be a constant [see Eq. (1)]. However, the Adam-Gibbs relation has been tested around T_g; therefore, to a good approximation, we can fix $\mathcal{E}$ to be a constant equal to

its $T = T_g$ value. The parameter D is inversely proportional to the fragility m: therefore, $m \sim \Sigma / \mathcal{E}$. Thus, fragility is not simply correlated to the total number of states: if the "barrier heights" grow faster than the total number of states, fragility can be a decreasing function of Σ. We will now show that this is indeed the case in the considered models.

C. Barrier heights, total number of states, and fragility

From Figs. 4 and 6 we see that the barrier height is indeed an increasing function of p in the considered models. Using Eq. (9), Eq. (18) can be written as

$$D = \mathcal{C} \frac{T_g}{T_K}. \tag{19}$$

Therefore, from Figs. 2 and 5 we see that D is indeed an increasing function of p that diverge for $p \to \infty$, as the ratio T_g / T_K increase on increasing p for both models. Thus, we can conclude that in the considered models the height of the barriers (in units of T_K) increases faster than the total number of states. This explains why one observe an inverse correlation between fragility and the total number of states, as discussed above and in Ref. [1].

D. Geometric picture of the phase space

Collecting all the information that we obtained in the previous sections, we can propose a geometric picture of the variation with p of the p-spin-model free-energy landscape. Indeed, on increasing p, (i) the total number of states increases, (ii) the volume of the states decreases (α decreases), and (iii) the height of the barriers between states increases.

Thus, we get the picture of a landscape where, on increasing p, a great number of small states with very high curvatures and separated by very high barriers appear: a sketch of this evolution is given in Fig. 9. The behavior of the fragility in this situation is related to the behavior of $\Sigma / \mathcal{E}$, the ratio between number of states and height of the barriers between them: in these models, it turns out that $\mathcal{E}$ increases faster than
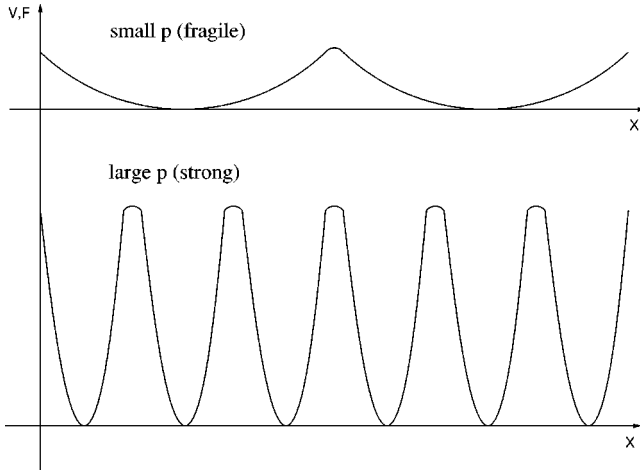
FIG. 9. Sketch of the evolution of the p-spin free energy by varying p: at small p there is a small number of states of large volume separated by low barriers; at high p there is a large number of states of small volume separated by high barriers. The height of the barriers increases faster than the number of states: thus, fragility is a decreasing function of p.

Σ, and the fragility is a decreasing function of p.

This behavior is consistent with the fact that fragility turns out to be positively correlated with the "volume" of the states as measured by α. Indeed, if, on the contrary, the barrier height grew slower than the total number of states (equivalently, if m were positively correlated with the total number of states), there should be also an inverse correlation between m and α, in disagreement with what is experimentally observed.

In the $p \to 2$ limit, where the fragility becomes infinite, the second derivative with respect to q of the potential $V(q,T)$ calculated in $q=0$ and $T=T_K=T_d$ vanishes (see Fig. 1) and the so-called spin glass susceptibility diverges at the critical temperature. In other words, when the fragility becomes infinite soft modes appear at the critical temperature, supporting the previously presented physical picture.

Note that the outlined picture is valid for "Gaussian-like" models—i.e., models where the complexity is a concave function of the temperature that vanishes at T_K without any inflection point. These models seem to describe correctly the distribution of basins in real systems only for relatively high fragilities. The behavior of the complexity (or configurational entropy, or excess entropy) as a function of temperature for very strong systems is still an open problem; our discussion may not apply to these systems.

VI. CONCLUSIONS

From the investigation of two mean-field p-spin models, we proposed a picture for the evolution of the free-energy landscape from fragile liquids to strong ones. This picture accounts for the recently observed correlation between fragility of a liquid and vibrational properties of the corresponding glass. The main prediction of our analysis is that the total number of states and the Adam-Gibbs parameter $\mathcal{E}$ should both be decreasing functions of the fragility. Unfortunately,

existing data are not sufficient to strictly test this prediction; excess entropy is available only for a few experimental systems, and numerical simulations are performed in a temperature range where the fragility of the investigated systems is approximately the same. We hope that these predictions can be tested in the future.

APPENDIX: THE TWO-REPLICA POTENTIAL

The two-replica potential is defined in Ref. [9] as

$$V(q) = -F(T) - \frac{T}{N} \int d\sigma \frac{e^{-\beta H(\sigma)}}{Z(\beta)} \ln Z(\sigma, q),$$

$$\tag{A1}$$

$$Z(\sigma, q) = \int d\tau e^{-\beta H(\tau)} \delta(q - q(\sigma, \tau)),$$

where $F(T)$ is the equilibrium free energy and $q(\sigma, \tau)$ is the overlap function. The following expression is then derived [18]:

$$V(q) = -F(T) - \lim_{n \to 0} \lim_{m \to 1} \frac{T}{Nn} \frac{\partial}{\partial m} \left(\int d\sigma e^{-\beta H(\sigma)} Z(\sigma, q)^{m-1} \right)^n.$$

$$\tag{A2}$$

The last integral can be rewritten as

$$\left(\int d\sigma e^{-\beta H(\sigma)} Z(\sigma, q)^{m-1} \right)^n$$

$$= \int d\sigma_{a\alpha} e^{-\beta \sum_{a\alpha} H(\sigma_{a\alpha})} \prod_{a=1}^{n} \prod_{\alpha=2}^{m} \delta(q - q(\sigma_{a1}, \sigma_{a\alpha})),$$

$$\tag{A3}$$

where $a = 1, \cdots, n$, $\alpha = 1, \cdots, m$. This is exactly the expression of the nm-times-replicated equilibrium partition function, with the additional constraint given by the δ functions. Using standard manipulations [12], it is rewritten as

$$\int dQ_{a\alpha,b\beta} e^{Nf(Q)} \prod_{a=1}^{n} \prod_{\alpha=2}^{m} \delta(q - Q_{a1,a\alpha}),$$

$$\tag{A4}$$

$$f(Q) = \frac{\beta^2}{4} \sum_{a\alpha,b\beta} Q_{a\alpha,b\beta}^p + \frac{1}{2} \ln \det Q.$$

Thus, evaluating the integral at the saddle point, we get

$$V(q) = -F(T) - \lim_{n \to 0} \lim_{m \to 1} \frac{T}{n} \frac{\partial}{\partial m} f(\overline{Q}). \tag{A5}$$

The matrix $\overline{Q}$ is defined by the following conditions:
(i) The elements on the diagonal are equal to 1.
(ii) The elements $\overline{Q}_{a1a\alpha}$, $\alpha > 1$, are equal to q.

(iii) All the other elements are determined by maximization of $f(Q)$.

As usual, one needs a parametrization of the matrix Q in order to perform the analytic continuation to noninteger n and m. A possible ansatz is [9] (in the example, $n=3$, $m=4$):

$$\overline{Q} = \begin{pmatrix} \begin{pmatrix} 1 & q & q & q \\ q & 1 & r & r \\ q & r & 1 & r \\ q & r & r & 1 \end{pmatrix} & 0 & 0 \\ 0 & \begin{pmatrix} 1 & q & q & q \\ q & 1 & r & r \\ q & r & 1 & r \\ q & r & r & 1 \end{pmatrix} & 0 \\ 0 & 0 & \begin{pmatrix} 1 & q & q & q \\ q & 1 & r & r \\ q & r & 1 & r \\ q & r & r & 1 \end{pmatrix} \end{pmatrix}.$$

Within this ansatz and using the relation

$$\det \begin{pmatrix} 1 & q & q & q \\ q & 1 & r & r \\ q & r & 1 & r \\ q & r & r & 1 \end{pmatrix} = (1-r)^{m-2}[1-2r+rm-(m-1)q^2],$$

(A6)

one gets

$$V(q) = -\frac{\beta q^p}{2} + \frac{\beta r^p}{4} - \frac{T}{2}\left[\ln(1-r) + \frac{r-q^2}{1-r}\right], \quad \text{(A7)}$$

where $r(q)$ is determined by $\partial_r V=0$. Now, it is easy to check that the condition $dV/dq=\partial_q V=0$, together with $\partial_r V=0$, is satisfied if $q=r$. Thus, when $V(q)$ is stationary, $r(q)=q$ and the potential $V(q)$ reduces to the one given by Eq. (15).

The fact that when $dV/dq=0$ the matrix Q reduces to the usual 1RSB overlap matrix (let us call it $\mathcal{Q}$) is general: indeed, the condition dV/dq from Eq. (A5) is equivalent to

$$\frac{df(Q)}{dQ} = 0. \qquad \text{(A8)}$$

This means that the function $f(Q)$ must be stationary with respect to all elements of Q if $dV/dq=0$, and we know that the 1RSB matrix $\mathcal{Q}$ provides a solution to this condition. As a final remark, we note that if $\overline{Q}=\mathcal{Q}$, we have

$$\frac{f(\overline{Q})}{nm} = -\beta\varphi_{1RSB}(m,q), \qquad \text{(A9)}$$

where φ_{1RSB} is the usual 1RSB free energy. Substituting this expression in Eq. (A5), one obtains

$$V(q) = -F(T) + \lim_{m\to 1}\partial_m(m\varphi_{1RSB}(m,q))$$

$$= \lim_{m\to 1}\partial_m\varphi_{1RSB}(m,q), \qquad \text{(A10)}$$

using the relation $\varphi_{1RSB}(m=1)=F(T)$ which holds above T_K. Therefore, *on its stationary points*, $V(q)$ is given (at the 1RSB level) by this simple expression, which can be easily calculated in several models. Note that, as discussed in Ref. [14], full RSB effects can be important for the computation of $V(q)$. However, we do not account for them in this paper.

[1] G. Ruocco, F. Sciortino, F. Zamponi, T. Scopigno, and C. De Michele, J. Chem. Phys. (to be published), e-print cond-mat/0401449.

[2] L.-M. Martinez and C. A. Angell, Nature (London) **410**, 663 (2001).

[3] K. Ngai, J. Non-Cryst. Solids **275**, 7 (2000).

[4] A. P. Sokolov, E. Rössler, A. Kisliuk, and D. Quitmann, Phys. Rev. Lett. **71**, 2062 (1993); S. Yannopoulos and G. Papatheodorou, Phys. Rev. B **62**, 3728 (2000).

[5] R. Hall and P. Wolynes, J. Chem. Phys. **86**, 2943 (1987); J. C. Dyre and N. B. Olsen, Phys. Rev. Lett. **91**, 155703 (2003).

[6] T. Scopigno, G. Ruocco, F. Sette, and G. Monaco, Science **302**, 849 (2003).

[7] L. F. Cugliandolo, in *Slow Relaxation and Nonequilibrium Dynamics in Condensed Matter*, edited by J.-L. Barat *et al.* (Springer-Verlag, Berlin, 2002).

[8] F. H. Stillinger and T. A. Weber, Phys. Rev. A **28**, 2408 (1983); S. Sastry, J. Phys.: Condens. Matter **12**, 6515 (2000); S. Corezzi, L. Comez, and D. Fioretto, e-print cond-mat/0211379; D. Prevosto, M. Lucchesi, S. Capaccioli, R. Casalini,

and P. A. Rolla, Phys. Rev. B **67**, 174202 (2003).

[9] S. Franz and G. Parisi, J. Phys. I **5**, 1401 (1995).

[10] S. Franz and G. Parisi, Phys. Rev. Lett. **79**, 2486 (1997).

[11] A. Cavagna, I. Giardina, and G. Parisi, J. Phys. A **30**, 7021 (1997).

[12] A. Crisanti and H. J. Sommers, Z. Phys. B: Condens. Matter **87**, 341 (1992); **92**, 257 (1993).

[13] A. Crisanti and H. J. Sommers, J. Phys. I **5**, 805 (1995).

[14] A. Barrat, S. Franz and G. Parisi, J. Phys. A **30**, 5593 (1997).

[15] B. Derrida, Phys. Rev. Lett. **45**, 79 (1980); Phys. Rev. B **24**, 2613 (1981).

[16] T. R. Kirkpatrick and P. G. Wolynes, Phys. Rev. A **35**, 3072 (1987); T. R. Kirkpatrick and D. Thirumalai, Phys. Rev. Lett. **58**, 2091 (1987); T. R. Kirkpatrick, D. Thirumalai and P. G. Wolynes, Phys. Rev. A **40**, 1045 (1989).

[17] P. G. Debenedetti and F. H. Stillinger, Nature (London) **410**, 259 (2001); R. J. Speedy, J. Phys. Chem. B **103**, 4060 (1999); S. Sastry, Nature (London) **409**, 164 (2001).

[18] Note that the expression given in [9], Eq. (15), is slightly different from this one probably due to a typographical error.